Monthly Notices
of the
ROYAL ASTRONOMICAL SOCIETY

Mon. Not. R. Astron. Soc. **414,** 489–494 (2011) doi:10.1111/j.1365-2966.2011.18409.x

Magnetospheric activity of bare strange quark stars

J. W. Yu★ and R. X. Xu★

School of Physics and State Key Laboratory of Nuclear Physics and Technology, Peking University, Beijing 100871, China

Accepted 2011 January 23. Received 2011 January 16; in original form 2010 December 5

ABSTRACT

In the model of Ruderman and Sutherland, the binding energy problem is a severe problem when modelling normal neutron stars as pulsars, i.e. both ions (e.g. $^{56}_{26}$Fe) and electrons on the normal neutron star surface can be pulled out freely by the unipolar generator induced electric field, so that sparking on the polar cap can hardly occur. This problem can be solved within the partially screened gap (PSG) model for neutron stars. However, in this paper, we study this problem extensively in a model of bare strange quark stars (BSSs). We find that the huge potential barrier built by the electric field in the vacuum gap above the polar cap can usually prevent electrons from streaming into the magnetosphere, unless the electric potential of a pulsar is sufficiently lower than that at the infinite interstellar medium. Other processes, such as the diffusion and thermionic emission of electrons, have also been included here. Our conclusions are as follows. Both positive and negative particles on the surface of a BSS are bound strongly enough to form a vacuum gap above its polar cap as long as the BSS is not charged (or not highly negative charged), and multi-accelerators can occur in the magnetosphere of the BSS. Our results may be helpful to distinguish normal neutron stars and bare quark stars using a pulsar's magnetospheric activities.

Key words: elementary particles – star: neutron – pulsars: general.

1 INTRODUCTION

Although pulsar-like stars have many different manifestations, they are populated mainly by rotation-powered radio pulsars. Much information about the pulsar radiative process is inferred from the integrated and individual pulses, the subpulses and even the microstructures of radio pulses. Among the magnetospheric emission models, the user-friendly nature of the model of (hereafter RS75 Ruderman & Sutherland 1975) is a virtue not shared by others (Shukre 1992).

In the RS75 model and its modified versions (e.g. Qiao & Lin 1998), a vacuum gap exists above the polar cap of a pulsar, in which charged particles (electrons and positrons) are accelerated because $\boldsymbol{E} \cdot \boldsymbol{B} \neq 0$. These accelerated charged particles, moving along the curved magnetic field lines, radiate curvature or inverse-Compton-scattering-induced high-energy photons, which are converted to $e^{\pm}$ while propagating in a strong magnetic field. A follow-up breakdown of the vacuum gap produces secondary electron–positron pair plasma that radiates coherent radio emission. These models with gap-sparking provide a good framework in which to analyse observational phenomena, especially drifting (Drake & Craft 1968; Deshpande & Rankin 1999; Vivekanand & Joshi 1999) and bi-drifting (Qiao et al. 2004) subpulses.

However, vacuum gap models that are like the RS75 model work only under strict conditions: a strong magnetic field and low temperature on the surface of pulsars (e.g. Medin & Lai 2007; Gil et al. 2008). The binding energy of positive ions (e.g. $^{56}_{26}$Fe) necessary for the RS75 model to work should be higher than $\sim$10 keV. However, calculations have shown that the cohesive energy of $^{56}_{26}$Fe at the neutron star surface is $<$1 keV (Fowlers et al. 1977; Lai 2001). This binding energy problem can be solved within a partially screened inner gap model (Gil, Melikidze & Geppert 2003; Gil, Melikidze & Zhang 2006a; Melikidze & Gil 2009) for normal neutron stars. Alternatively, it is noted that the binding energy can be sufficiently high if pulsars are bare strange quark stars (BSSs; Xu & Qiao 1998; Xu, Qiao & Zhang 1999; Xu, Zhang & Qiao 2001), although strange stars were previously supposed to exist with crusts (Alcock, Farhi & Olinto 1986). Certainly, it is very meaningful in the elementary strong interaction between quarks and the phases of cold quark matter that the binding energy problem can be solved by bare quark stars as pulsars (Xu 2009, 2010).

Although the ideas of solving the binding energy problem in BSS model have been presented and discussed in some studies, up to now there has been no comprehensive study with quantitative calculations. In this paper, we investigate the BSS model in quantitative detail and we show the physical picture of the binding of particles on the surface of a BSS. Our research shows are that multi-accelerators could occur above the polar cap for (and only for) curvature-radiation-induced (CR-induced) sparking normal pulsars (NPs). However, for other cases, such as resonant

★E-mail: J.W.Yu@pku.edu.cn (JWY); r.x.xu@pku.edu.cn (RXX)

inverse-Compton-scattering-induced (ICS-induced) sparking NPs and both CR-induced and ICS-induced millisecond pulsars (MSPs), particles on the surface of BSSs are bound strongly enough to form a vacuum gap and models like the RS75 model work well if pulsars are BSSs.

2 ACCELERATORS ABOVE THE POLAR CAPS OF BARE STRANGE QUARK STARS

On the surface of a BSS, there are positively (u-quarks) and negatively (d- and s-quarks and electrons) charged particles. Quarks are confined by strong colour interaction, whose binding energy can be considered as infinity when compared with the electromagnetic interaction, while electrons are bound by electromagnetic interaction. Therefore, in this paper we focus on the binding of electrons.

First, let us discuss briefly the binding of electrons in the BSS model. On one hand, assuming the electric potential at the top of the RS75 vacuum gap is the same as that of the interstellar medium, we could then have a potential barrier for electrons by integrating the gap electric field from top to bottom in the vacuum gap. This potential barrier could then prevent electrons streaming into the magnetosphere. On the other hand, electrons above the stellar surface of a BSS are described in the Thomas–Fermi model, in which the total energy of electrons on the Fermi surface would be a constant, ϕ_0. In previous work (e.g. Alcock et al. 1986), this constant was chosen to be zero, $\phi_0 = 0$, because the effect of a spinning BSS with strong magnetic fields was not considered. Because of the unipolar generator effect, the potential drop between different magnetic field lines is set up from pole to equatorial plane. This potential drop could result in different ϕ_0, at different polar angle, θ. The total energy of electrons would then be obtained by choosing a certain zero potential magnetic field line (i.e. at $\theta_{\rm B}$ or $\theta_{\rm C}$ in Fig. 1). Finally, by comparing the total energy of electrons with the height of the potential barrier in the vacuum gap, we can see whether electrons can stream into the magnetosphere freely or not.

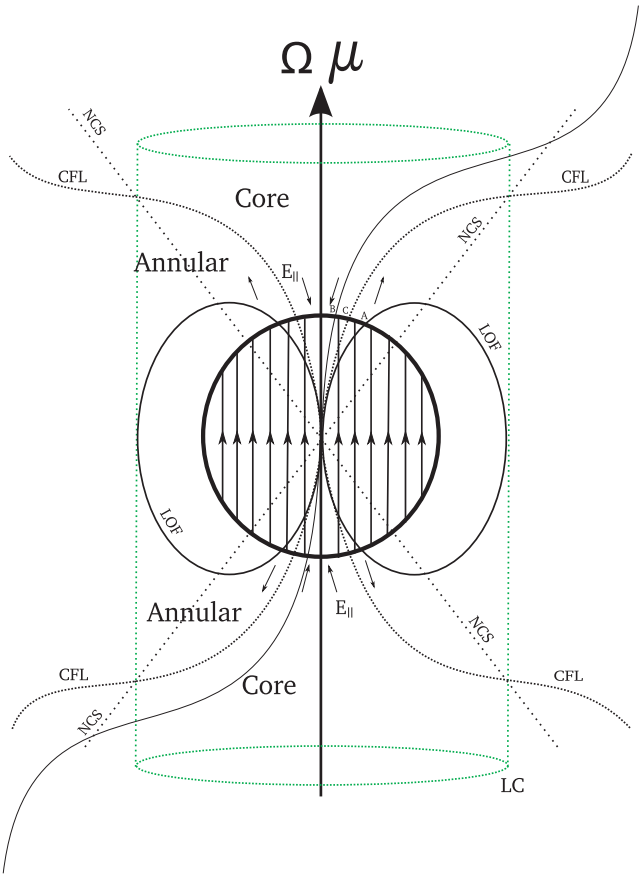

Figure 1. A schematic representation of the geometry of 'antipulsars'. CFL stands for the critical field lines, NCS for the null charge surface and LC for light cylinder. The enlarged arrows with opposite directions in the annular region and core region represent the directions of the electric field in the vacuum gap. 'A', 'B' and 'C' represent the feet of the different magnetic field lines (see text).

2.1 Energy of electrons on the Fermi surface

The distribution of electrons in BSSs is described in the Thomas–Fermi model (Alcock et al. 1986). In this model, the equilibrium of electrons in an external electric field ensures that the total energy of each electron on Fermi surface is a constant, ϕ_0. For the case of extremely relativistic degenerate electron gas, this gives (Alcock et al. 1986)

$$\epsilon(\boldsymbol{r}) = cp_{\rm F}(\boldsymbol{r}) - e\varphi(\boldsymbol{r}) = \phi_0. \quad (1)$$

Here, $\epsilon(\boldsymbol{r})$ is the total energy, $cp_{\rm F}(\boldsymbol{r})$ is the Fermi energy, $-e\varphi(\boldsymbol{r})$ is the electrostatic potential energy of electrons and ϕ_0 is a constant, describing the potential energy of electrons in the Thomas–Fermi model at infinity.

However, the potential distribution of electrons on the star's surface as a result of the electric field induced by the rotating, uniformly magnetized star, for the sake of simplicity, could be assumed and estimated as (see equation 2 of Xu, Cui & Qiao 2006)

$$V_{\rm i}(\theta) \simeq 3 \times 10^{16} B_{12} R_6^2 P^{-1} \sin^2\theta \ ({\rm V}) + V_0. \quad (2)$$

Here, $B_{12} = B/(10^{12}\,{\rm G})$ and $R_6 = R/(10^6\,{\rm cm})$ is the radius of a pulsar, $P = 2\pi/\Omega$ is the pulsar period, θ is the polar angle and V_0 is another constant. Because the distribution of electrons above the surface of the BSS extends only thousands of femtometres, the macroscopic potential drop between different magnetic field lines can be thought to be at infinity in the Thomas–Fermi model. Also, the potential energy related to equation (2), $eV_{\rm i}$, can be regarded as the constant, ϕ_0, in equation (1). By choosing a certain zero potential magnetic field line, we can obtain the total energy of electrons, namely $eV_{\rm i}$. Two scenarios are possible here. The first scenario is that we choose the critical field lines whose feet are at the same electric potential of the interstellar medium (Goldreich & Julian 1969) as the zero potential. We also suggest a second choice in which the zero potential should be at those magnetic field lines that separate the annular and core regions determined by $S_{\rm AG} = S_{\rm CG}$ (where $S_{\rm AG}$ and $S_{\rm CG}$ are the stellar surface areas of the annular and core regions, respectively). The second scenario is based on the idea that if particles with opposite charge stream into the magnetosphere with $\rho_{\rm GJ}$ in both regions, the areas of these two regions should approximately be equal in order to keep the star from charging. The feet of the critical field lines and the magnetic field lines determined by $S_{\rm AG} = S_{\rm CG}$ are designated as C and B, respectively (Fig. 1). For the above two scenarios, the total energies, $\phi_{\rm i} = eV_{\rm i}$, of the electrons on the Fermi surface are given, respectively, by

$$\phi_{\rm i,C}(\theta) \simeq -3 \times 10^{10} B_{12} R_6^2 P^{-1} \left(\sin^2\theta - \sin^2\theta_{\rm C}\right)\ {\rm MeV}, \quad (3)$$

and

$$\phi_{\rm i,B}(\theta) \simeq -3 \times 10^{10} B_{12} R_6^2 P^{-1} \left(\sin^2\theta - \sin^2\theta_{\rm B}\right)\ {\rm MeV}. \quad (4)$$

Here, θ_C and θ_B are polar angles of C and B (see Fig. 1). Equations (3) and (4) imply that the total energy of electrons is higher at the poles and decreases towards the equator for an 'antipulsar' ($\boldsymbol{\Omega} \cdot \boldsymbol{B} > 0$), which means that electrons in different regions above a polar cap may behave differently.

2.2 Potential barrier of electrons in a vacuum gap

In the following, we consider the potential barrier of electrons in a vacuum gap. Unlike RS75, we perform calculations for the situation of an 'antipulsar' whose magnetic axis is parallel to its spin axis. A schematic representation of an 'antipulsar' is shown in Fig. 1. Assuming that the electric potential at the top of the RS75 vacuum gap is the same as that of the interstellar medium, we can obtain a potential barrier for electrons by integrating the gap electric field from top to bottom in the vacuum gap. This potential barrier, in a one-dimensional approximation, is (RS75)

$$\phi_p(Z) = 2\pi \times 10^4 P^{-1} B_{12}(h_3 - Z_3)^2 \text{ MeV}, \quad (5)$$

where $h_3 = h/(10^3 \text{ cm})$ is the height of the vacuum gap and $Z_3 = Z/(10^3 \text{ cm})$ is the space coordinate measuring the height above the quark surface. This potential barrier may prevent electrons from injecting into the pulsar's magnetosphere. The height of this potential barrier mainly depends on the height of the vacuum gap, which is determined by the cascade mechanics of sparking (i.e. the CR-induced cascade sparking and the ICS-induced cascade sparking). In the CR-induced cascade sparking model, the gap height is (RS75)

$$h_{CR} = 5 \times 10^3 \rho_6^{2/7} B_{12}^{-4/7} P^{3/7} \text{ cm}. \quad (6)$$

In the ICS-induced cascade sparking model, it is (Zhang, Harding & Muslimov 2000)

$$h_{ICS} = 2.79 \times 10^4 \rho_6^{4/7} B_{12}^{-11/7} P^{1/7} \text{ cm}. \quad (7)$$

In Gil et al. (2006a), the heights of the vacuum gap of both CR-induced and ICS-induced sparking mechanisms (see equations 21 and 22 of Gil et al. 2006a) are different from what we have used in this work. In the PSG model, there was a partial flow of iron ions from the positively charged polar cap, which coexist with the production of outflowing electron–positron plasmas. Such a charge-depleted acceleration region is also highly sensitive to both the critical ion temperature and the actual surface temperature of the polar cap (Gil et al. 2003). In contrast, in our model, there is no flow of positively charged particles (i.e. quarks), and also it is insensitive to the actual surface temperature. This means that there is no partial screened effect above the polar cap of bare strange quark stars (i.e. the pure vacuum gap exists on the polar cap of bare strange quark stars). This is the reason why we use equations (6) and (7) in our calculation. Whether this choice for the height of the vacuum gap can result in different drift rates of subpulses or not is a complicated problem. We discuss this problem very briefly in Section 3. The potential barrier of electrons in the gap for the CR-induced cascade sparking model of typical NPs is plotted in Fig. 2, in which the total energy of electrons at the stellar surface (i.e. ϕ_i) is illustrated at different polar angles. The situation of the CR-induced cascade sparking of typical MSPs is similar to that of NPs but with a greater height of the potential barrier.

By comparing the potential barrier with the total energy of electrons, we explain the behaviour of electrons above the polar cap. That is, only electrons with energy greater than the potential barrier can escape into the pulsar's magnetosphere. It is known that the energy of electrons is a function of the polar angle (equations 3 and 4). As a result, there may be a critical polar angle, θ_0, at which the energy of electrons equals the height of this potential barrier. Fig. 3 shows a comparison between the total energy of electrons and the height of the potential barrier on the stellar surface for typical NPs of CR-induced sparking (θ_0 does not exist for the ICS-induced sparking of both NPs and MSPs; see Table 1). The results are as follows. Free flow status stays in the region of $[0, \theta_0]$ and the vacuum gap in $[\theta_0, \theta_A]$ for 'antipulsars', where θ_A is the polar angle of the feet of the last open field lines (Fig. 1). We give the results of θ_0 in Table 1 for both the pulsar and 'antipulsar'. We find that for the special case of CR-induced sparking NPs, the free flow and vacuum gap could coexist above the polar cap, which is different from the previous scenario. The general case is that only the vacuum gap exists.

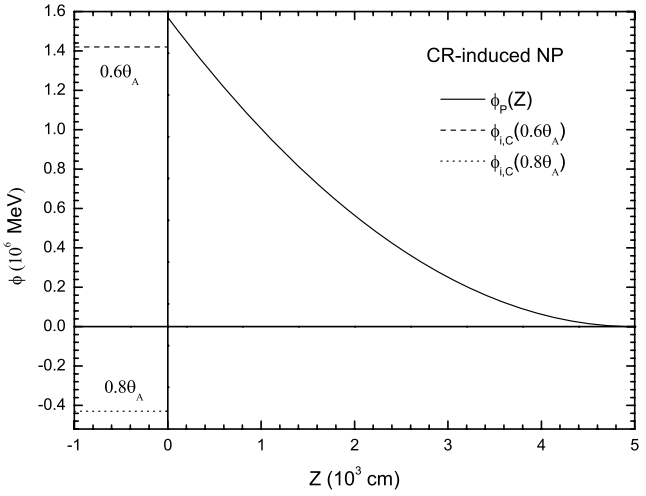

Figure 2. Potential barrier of electrons, ϕ_P, in the vacuum gap of typical NPs ($P = 1$ s, $B = 10^{12}$ G). The potential energy of electrons at the stellar surface, $\phi_i(\theta)$, is illustrated with fixed polar angles (e.g. with $0.6\theta_A$ and $0.8\theta_A$), where θ_A is the polar angle of the feet of the last open field lines (see Fig. 1).

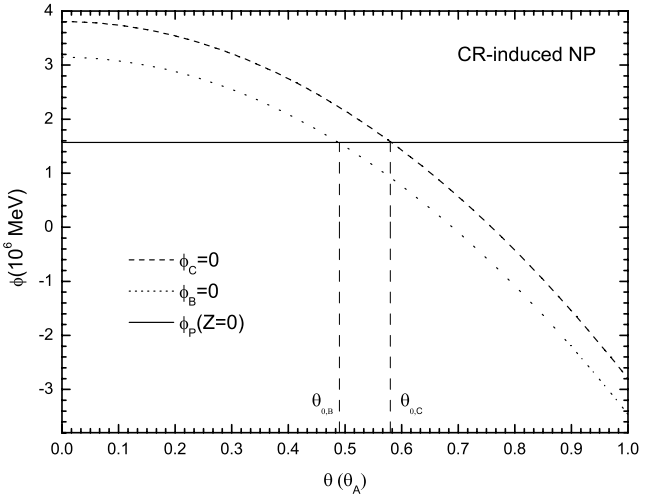

Figure 3. Comparison between the total energy of electrons on the stellar surface with the height of the potential barrier of typical NPs with $\phi_i(\theta_C) = 0$ and $\phi_i(\theta_B) = 0$, respectively. The solid horizontal line is the height of the potential barrier of electrons, $\phi_P(Z = 0)$.

Table 1. Polar angles of θ_B, θ_C and θ_0 for both CR-induced and ICS-induced sparking of typical NPs and MSPs within both choices of zero potentials.

	θ_A (rad)	$\theta_B(\theta_A)$	$\theta_C(\theta_A)$	$\theta_{0,B}(\theta_A)$ CR	$\theta_{0,B}(\theta_A)$ ICS	$\theta_{0,C}(\theta_A)$ CR	$\theta_{0,C}(\theta_A)$ ICS	
				0.49	–[a]	0.58	–	$\boldsymbol{\Omega}\cdot\boldsymbol{B}>0$
NPs	0.0145	0.69	0.76	0.84	2.76[b]	0.90	2.83[b]	$\boldsymbol{\Omega}\cdot\boldsymbol{B}<0$
				–	–	–	–	$\boldsymbol{\Omega}\cdot\boldsymbol{B}>0$
MSPs	0.145	0.69	0.76	1.49[2]	–	1.52[2]	–	$\boldsymbol{\Omega}\cdot\boldsymbol{B}<0$

[a] θ_0 does not exist, which means that the whole polar cap region is a vacuum gap.
[b] $\theta_0 > \theta_A$, which means that the whole polar cap region is a vacuum gap.

2.3 Effects of thermionic emission and diffusion of electrons

It follows from the previous argument that electrons inside BSSs usually cannot stream into magnetospheres. Are there any other processes that can affect the existence of the vacuum gap above the polar cap? In the vacuum gap, except for the pulling of electrons from the interior of the BSS, there are two other processes to be investigated, which could also prevent the vacuum gap from being formed: the thermionic emission of electrons and the diffusion of electrons from the outer edge to the inner region of the polar cap. For the first process, if the current density resulting from thermionic emission of electrons is much smaller than that of the Goldreich–Julian charge density, the vacuum gap can also be maintained. This current density is determined by the Richard–Dushman equation (Usov & Melrose 1995)

$$J_{\rm th} = 1.2\times10^{14}T_6^2\exp!\left(-1.161\times10^4T_6^{-1}\phi_{\rm MeV}\right)\ {\rm A\,cm^{-2}}, \quad (8)$$

where m_e is the electron mass, k_B is the Boltzmann constant, $T_6 = T/(10^6\ {\rm K})$ is the temperature and $\phi_{\rm MeV} = \phi/{\rm MeV}$ is the work function of electrons. In the vacuum gap of BSSs, the work function of thermionic electrons is the order of the difference between the height of the potential barrier and the total energy of electrons at the surface of the BSS. The order of the difference is about 10^6 MeV. At the same time, the surface temperature of the polar caps of BSSs is of the order of 10^6 K. Thus, the thermionic emission current density is $\sim$0, which means that the thermionic emission of electrons cannot affect the existence of the vacuum gap.

The second process is the diffusion of electrons whose distribution above the surface of a BSS is (Xu et al. 2001)

$$n_e(Z) = \frac{1.187\times10^{32}\phi_{\rm q,MeV}^3}{(0.06\phi_{\rm q,MeV}Z_{11}+4)^3}\ {\rm cm^{-3}}. \quad (9)$$

Equation (9) implies that the number density of electrons (and the kinetic energy density, ϵ_k) decreases rapidly with an increase of the distance from the quark matter surface at which $\epsilon_k \gg \epsilon_B$ (where ϵ_B is the magnetic field energy density). As a result, there is a balanced surface where the kinetic energy density equals the magnetic energy density. Below this balanced surface, electrons can cross the magnetic field lines freely; above the balanced surface, this motion is prevented. The physical picture of the diffusion of electrons is illustrated in Fig. 4. Making use of $\epsilon_k = \epsilon_B$, where $\epsilon_k = n_e\epsilon_F$ (ϵ_F is the Fermi energy of degenerate electrons) and $\epsilon_B = B^2/8\pi$, we can obtain the height of the balanced surface. For NPs, this is $Z_{11}\simeq160$ and for MSPs, it is $Z_{11}\simeq1.7\times10^4$, where $Z_{11} = Z/(10^{-11}\ {\rm cm})$. Note that there is a directed outward surface electric field above the quark matter surface. This surface electric field is much stronger than the gap electric field, but it decreases rapidly with an increase of the distance. This means that the surface electric field becomes smaller than the gap electric field above a certain distance, $Z_{0,11}$. For NPs, this is $Z_{0,11}\simeq7000$, and for MSPs, it is $Z_{0,11}\simeq6.3\times10^6$ (see Fig. 4). For both the NPs and MSPs, we have $Z_{11}\ll Z_{0,11}$. The diffusion of electrons beneath $Z_{0,11}$ is still confined by the surface electric field, which means that it is only necessary to consider the diffusion of electrons above the surface with a height of $Z_{0,11}$. The diffusion coefficient, D_c, is given by (Xu et al. 2001)

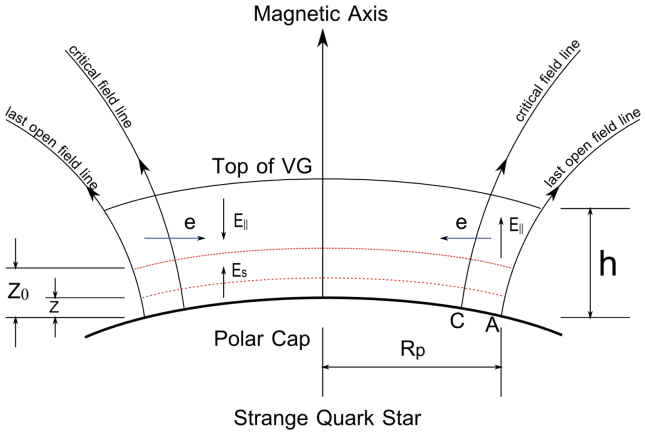

Figure 4. A representative illustration of the diffusion of electrons above the polar cap of a bare strange quark star.

$$D_c \simeq \frac{\rho^2}{\tau_F} = \frac{\pi n_e c e^2}{B^2} = 2.17\times10^{-3}B_{12}^{-2}n_{e,29}\ {\rm cm^2\,s^{-1}}, \quad (10)$$

where $\rho = \gamma\rho_L[\rho_L = m_e vc/(eB)$ is the Larmor radius] is the cyclotron radius of relativistic electrons, and $\tau_F \simeq \gamma m_e^2 v^3/(\pi e^4 n_e)$ is the mean-free flight time of electrons. The gradient of electrons along with the diffusion direction is approximately

$$\frac{{\rm d}n_e}{{\rm d}x} \simeq \frac{n_e}{\rho} = 1.4\times10^{38}n_{e,29}^{2/3}\ {\rm cm^{-4}}. \quad (11)$$

Then, the diffusion rate is

$$I_{\rm df} = 2.77\times10^{29}B_{12}^{-1}P^{-1/2}R_6^{3/2}\int_{Z_{0,11}}^{\infty} n_{e,29}^{5/3}\,{\rm d}Z_{11}\ {\rm s^{-1}}, \quad (12)$$

where $n_{e,29} = n_e/(10^{29}\ {\rm cm^{-3}})$. For both NPs and MSPs with different ϕ_q, we give the results of the diffusion rate $I_{\rm df}$ and $I_{\rm GJ}$ in Table 2,

Table 2. Typical value of the diffusion rate for NPs and MSPs with different choices of ϕ_q.

	NPs		MSPs	
ϕ_q (MeV)	$I_{\rm df}$ (10^{24} s^{-1})	$I_{\rm GJ}$ (10^{24} s^{-1})	$I_{\rm df}$ (10^{17} s^{-1})	$I_{\rm GJ}$ (10^{17} s^{-1})
1	$\sim$4.75		$\sim$7.52	
10	$\sim$4.91	$\sim1.4\times10^3$	$\sim$7.52	$\sim1.4\times10^{13}$
20	$\sim$4.93		$\sim$7.53	

Table 3. Accelerators above the polar caps of BSSs.

	$[0, \theta_0]^a$		$[\theta_0, \theta_A]$		
	CR	ICS	CR	ICS	
	SCLF	VG	VG	VG	$\boldsymbol{\Omega} \cdot \boldsymbol{B} > 0$
NPs	VG	VG[b]	SCLF	VG[b]	$\boldsymbol{\Omega} \cdot \boldsymbol{B} < 0$
	VG	VG	VG	VG	$\boldsymbol{\Omega} \cdot \boldsymbol{B} > 0$
MSPs	VG[b]	VG	VG[b]	VG	$\boldsymbol{\Omega} \cdot \boldsymbol{B} < 0$

[a] θ_0 represents $\theta_{0,B}$ when choosing $\phi_B = 0$ and $\theta_{0,C}$ when choosing $\phi_C = 0$.
[b] For such cases, $\theta_0 > \theta_A$, which represents the structure of the whole polar cap region.

where the flow with the Goldreich–Julian flux is $I_{GJ} = \pi r_p^2 c n_{GJ} \simeq 1.4 \times 10^{30} P^{-2} R_6^3 B_{12}$ s^{-1}. We know that for both the NPs and MSPs, $I_{df} \ll I_{GJ}$ according to Table 2. This means that the diffusion of electrons is also negligible, which guarantees the existence of the vacuum gap.

3 DISCUSSION AND CONCLUSIONS

In the RS75 model, the binding energy problem is one of the most serious problems in the normal neutron star model of pulsars. Aron & Scharlemann (1979) have developed an alternative model, the space-charge limited flow (SCLF) model, in which the particles, both iron ions and electrons, can be pulled out freely to form a steady flow (Aron & Scharlemann 1979). In this SCLF model, the drifting subpulse phenomenon, which has been commonly observed in pulsars, can rarely be reproduced. The prerequisite for understanding this phenomenon could be the existence of a vacuum gap.

In a very special case, through our calculations, we find that there is a new physical scenario for the CR-induced sparking of NPs, in which the free flow and vacuum gap may coexist above the polar cap. However, in other cases, such as the ICS-induced sparking of NPs and MSPs, only the vacuum gap exists. In general, if a pulsar is not highly negatively charged (Xu et al. 2006), the vacuum gap also survives at the polar cap. One limitation is that our calculation is based on the one-dimensional approximation and it might fail in some cases for MSPs. As far as we know, it is very difficult to deal with high-dimensional cases. The one-dimensional approximation provides a good understanding of the geometry of the polar cap of a BSS. In conclusion, the binding energy problem can be solved completely in the BSS model of pulsars as long as the BSSs are neutral (or not highly negative charged), and the structure of the polar cap of BSSs is very different with respect to that of NSs. Detailed information about the geometry of the polar cap of BSSs is given in Table 3. A more interesting region from the pole to the equator can be located between the polar angle where the total energy of electrons equals the potential barrier and the polar angle of the foot of the zero potential magnetic field line [i.e. $(\theta_{0,C}, \theta_C)$ or $(\theta_{0,B}, \theta_B)$; see Fig. 3] for CR-induced sparking NPs. After the birth of a NP, a vacuum gap exists at this region. When sparking starts, the potential in the vacuum gap drops rapidly because of screening by electron–positron pairs. It may become lower than that at the surface, namely $V_i(\theta)$. As a result, the sparking converts the vacuum gap to free flow at this region until the sparking ends [i.e. at $(\theta_{0,C}, \theta_C)$ or $(\theta_{0,B}, \theta_B)$, the vacuum gap and free flow work alternately]. This argument may have profound implications for us when we wish to distinguish neutron stars and quark stars using the magnetospheric activities of a pulsar (e.g. the diverse pulse profiles).

Another issue to be discussed concerns the drifting rate of subpulses when we use the height of the pure vacuum gap in this work. The drifting subpulse phenomenon in the vacuum gap can be explained naturally by $\boldsymbol{E} \times \boldsymbol{B}$. Unfortunately, these theoretical calculations have given a higher drifting rate with respect to observations (e.g. Ruderman & Sutherland 1975; Deshpande & Rankin 1999, 2001; Gil et al. 2003; Gil, Melikidze & Zhang 2006b). Since it was first observed (Drake & Craft 1968), the drifting subpulse phenomenon has remained unclear. It has been widely regarded as one of the most critical and potentially insightful aspects of pulsar emission (Deshpande & Rankin 2001). The PSG mechanism (e.g. Gil et al. 2003, 2006a,b) could be a way to understand the lower drifting rates observed, but some complexities still exist. This means that the underlying physics of drifting subpulses remains complicated and is far from being clear.

(i) In principle, the drifting velocity of subpulses is the ratio of the drifting distance to the duration, while the expected velocity predicted by $\boldsymbol{E} \times \boldsymbol{B}$ is only for electrons in separated emission units, namely the plasma filaments. These two velocities would not be the same if the plasma filaments can stop after sparking. When sparking starts, the electric field in the vacuum gap vanishes because of screening by plasmas; when sparking ends, the electric field appears again. Thus, the calculated drifting velocity with $\boldsymbol{E} \times \boldsymbol{B}$ could be higher than that of observations.

(ii) The so-called aliasing effect. As we observe subpulses only once every rotation period, we cannot determine their actual speed. The main obstacles in the aliasing problem are the undersampling of subpulse motion and our inability to distinguish between subpulses, especially when the differences between subpulses formed by various subbeams are smaller than the fluctuations in subpulses from one single subbeam (van Leeuwen et al. 2003). Thus, in the future, it is very important for this to be studied in detail.

We assume that the potential energy related to equation (2), eV_i, is the constant, ϕ_0, in equation (1). This assumption is reasonable. For a uniformly magnetized, rotating conductor sphere, the unipolar generator will induce an electric field, which is a function of the polar angle, as described in equation (2). In the case of $\boldsymbol{\Omega} \cdot \boldsymbol{B} > 0$ (Fig. 1), the potential energy of electrons is highest at the polar region, which means that the electrons there could find it easier to escape. Alternatively, this conclusion can be quantitatively understood as follows. Because of the Lorentz force inside a star, more electrons are located at the polar region, so the Fermi energy of electrons is higher there and the electrons find it easier to escape into the magnetosphere.

ACKNOWLEDGMENTS

We thank Dr Kejia Lee and other members in the pulsar group of Peking University for their helpful and enlightened discussions. We also thank Professor Janusz Gil for his helpful comments and suggestions. JY is grateful to Dr Caiyan Li for her helpful assistance. The work is supported by the Natural Science Foundation of China (10973002,10935001), the National Basic Research Programme of China (grant 2009CB824800) and the John Templeton Foundation.

REFERENCES

Alcock C., Farhi E., Olinto A., 1986, ApJ, 310, 261
Arons J., Scharlemann E. T., 1979, ApJ, 231, 854
Deshpande A. A., Rankin J. M., 1999, ApJ, 524, 1008
Deshpande A. A., Rankin J. M., 2001, MNRAS, 322, 438

Drake F. D., Craft H. D., 1968, Nat, 220, 231
Fowlers E. G., Lee J. F., Ruderman M. A., Sutherland P. G., Hillebrandt W., Muller E., 1977, ApJ, 215, 291
Gil J., Melikidze G., I., Geppert U., 2003, A&A, 407, 315
Gil J., Melikidze G., Zhang B., 2006a, ApJ, 650, 1048
Gil J., Melikidze G., Zhang B., 2006b, ChJAS, 6, 105
Gil J., Haberl F., Geppert U., Zhang B., Melikidze G. Jr, 2008, ApJ, 686, 497
Goldreich P., Julian W. H., 1969, ApJ, 157, 869
Lai D., 2001, Rev. Mod. Phys., 73, 629
Medin Z., Lai D., 2007, MNRAS, 382, 1833
Melikidze G., Gil J., 2009, in Soonthornthum B., Komonjinda S., Cheng K. S., Leung K. C., eds, ASP Conf. Ser. Vol. 404, Eighth Pacific Rim Conference on Stellar Astrophysics. Astron. Soc. Pac., San Francisco, p. 131
Qiao G. J., Lin W., 1998, A&A, 333, 172
Qiao G. J., Lee K. J., Zhang B., Xu R. X., Wang H. G., 2004, ApJ, 616, 127
Ruderman M. A., Sutherland P. G., 1975, ApJ, 196, 51
Shukre C. S., 1992, in Hankins T. H., Rankin J. M., Gil J. A., eds, Proc. IAU Colloq. 128, Magnetospheric Structure and Emission Mechanisms of Radio Pulsars. Pedagogical Univ. Press, Zielona Gora, Poland, p. 412
Usov V. V., Melrose D. B., 1995, Australian J. Phys., 48, 571
van Leeuwen A. G. J., Stappers B. W., Ramachandran R., Rankin J. M., 2003, A&A, 399, 223
Vivekanand M., Joshi B. C., 1999, ApJ, 515, 398
Xu R. X., 2009, J. Phys. G: Nucl. Part. Phys., 36, 064010
Xu R. X., 2010, Int. J. Mod. Phys., D19, 1437
Xu R. X., Qiao G. J., 1998, Chin. Phys. Lett., 15, 934
Xu R. X., Qiao G. J., Zhang B., 1999, ApJ, 522, L109
Xu R. X., Zhang B., Qiao G. J., 2001, Astropart. Phys., 15, 101
Xu R. X., Cui X. H., Qiao G. J., 2006, Chin. J. Astron. Astrophys., 2, 217
Zhang B., Harding A. K., Muslimov A. G., 2000, ApJ, 531, L135

This paper has been typeset from a TEX/LATEX file prepared by the author.